

Determination of Na submonolayer adsorption site on Cu(111) by low-energy ion blockingR. Zhang,¹ B. Makarenko,¹ B. Bahrim,² and J. W. Rabalais^{1,2}¹*Department of Chemistry, University of Houston, Houston, Texas 77204, USA*²*Department of Chemistry and Physics, Lamar University, Beaumont, Texas 77710, USA*

(Received 13 August 2007; published 18 September 2007)

The structure of a submonolayer coverage of sodium adsorbed on a Cu(111) surface at room temperature has been investigated using time-of-flight scattering and recoiling spectrometry. The effect of the adsorbed Na atoms on the angular distribution of scattered 2 keV H⁺ ions is analyzed by molecular dynamics and scattering and recoiling imaging code simulations. It is shown that at a coverage $\theta=0.25$ monolayer, Na atoms preferentially populate the fcc threefold surface sites with a height of 2.7 ± 0.1 Å above the first-layer Cu atoms. At a lower coverage of $\theta=0.10$ ML, there is no adsorption site preference for the Na atoms on the Cu(111) surface.

DOI: [10.1103/PhysRevB.76.113407](https://doi.org/10.1103/PhysRevB.76.113407)

PACS number(s): 61.30.Hn, 61.18.Bn, 61.80.Lj

The adsorption and coadsorption of alkali metals on metal surfaces are of considerable interest in surface science due to both their fundamental importance and technological applications.^{1,2} Details of the adsorption of Na on Cu(111) have been revealed through experimental^{3–8} and theoretical studies.^{9–11} In low-energy electron diffraction (LEED) studies,^{4–6} either a $p(2\times 2)$ pattern^{4,5} or a ring pattern (less ordered phase)⁶ have been observed at a coverage of $\theta=0.25$. The coverage θ is defined as the ratio between the number of adsorbed Na atoms and the number of Cu atoms in the outermost substrate layer. In low-temperature scanning tunneling microscopy (STM) studies,^{7,8} a structure transition that included some intermediate phases, such as a mixing of $p(3\times 3)$ and $p(2\times 2)$ structures up to a coverage of $\theta=0.25$ with one Na atom per unit cell was suggested. However, the adsorption site preference of Na on Cu(111) has not yet been conclusively revealed experimentally. Contradicting results about the adsorption site have also been obtained from various theoretical calculations^{9–12} because the binding energy/atom between the hollow-site-centered site and the top-bridge site adsorption structures may be as small as 5 meV/atom at $\theta=0.25$.¹⁰ A technique that can resolve such a question must have ultrahigh surface sensitivity. Advances in dechanneling and blocking effects in low-energy ion scattering (LEIS) have the unique ability to analyze the structure of the outermost atomic layers of materials. In this work, the LEIS technique of time-of-flight scattering and recoiling spectrometry (TOF-SARS) (Ref. 13) has been used to determine the Na adsorption site and adsorption height at low coverage on a “smooth” Cu(111) surface.

Low keV hydrogen ions (H⁺) were used as the probing beam, with a typical accuracy of <0.1 Å for determination of interatomic spacings.¹³ Since the energy of the ions is in the keV regime, the scattering cross sections σ are substantially enhanced as compared with the meV scattering counterpart. Consequently, the ions can only penetrate into the shallow subsurface layers where dechanneling readily occurs. Scattering and recoiling imaging code (SARIC) simulations^{14–16} show that only the outermost four Cu layers of the Cu(111) surface can be “seen” by most of the incoming H ions. These Cu atoms serve as point scatters and give rise to a flux of scattered H particles that have experienced

only single or quasi-single collisions. The angular intensity distribution of the scattered H particles from these point scatters is nearly isotropic for large scattering angles.¹³ This type of isotropic outgoing flux can act as a very sensitive probe of the foreign atoms adsorbed in an ordered array on the crystal surface. When a Na atom is deposited onto a site in the vicinity of substrate Cu atoms (point scatters), it will block part of the scattered H trajectories from these Cu atoms so that the scattering intensity will exhibit minima at specific exit angles. These angles correspond to the direction of the interatomic axes between the Na and Cu atoms. As a result, the Na adsorption site and adsorption height can be determined by simple geometrical constructs. The adsorbed Na atoms can also perturb the incoming H atom trajectories, resulting in a change in the conservation of the number of scattered H atoms and making the interpretation more complicated. However, judicious choice of the scattering angle for the incident angle scans can eliminate this negative effect. A large scattering angle (100°) was used herein in order to eliminate such Na disturbances. Furthermore, it can advantageously use the Na atoms to focus incoming H ions onto the Cu scatters, thereby increasing the blocking effect. The three basic advantages of using low-energy ion blocking to quantitatively determine a chemisorption site are as follows: (i) No prerequisite knowledge of the actual shapes of the blocking cones is required; (ii) accurate values of σ are not necessary since only normalized yields rather than absolute yields are needed; and (iii) the positions of the adsorbed atoms can be derived unambiguously by a triangulation procedure using incident angle scans with proper large scattering angles. The spectral interpretation, as described elsewhere,^{17–19} is facilitated by use of (i) the simulation program SARIC,¹⁸ which is based on the classical theory of ion scattering using a binary collision approximation (BCA), and (ii) “two-atom” molecular dynamics (MD) simulations.²⁰

All measurements were carried out at room temperature in a TOF-SARS spectrometer that has been described in detail elsewhere.^{21–23} Briefly, the experiments were performed in an ultrahigh vacuum chamber with a base pressure of 5×10^{-10} Torr. The 2 keV H⁺ primary ion beam that was used for scattering from the Cu(111) target surface was pulsed at a rate of 50 kHz with a 50 ns pulse width and a 0.5 nA/cm² average ion flux. The velocities of the keV outgoing scat-

tered H atoms and ions were analyzed through a 90 cm long time-of-flight drift region and detected by two channel electron multiplier (CEM) detectors in the same scattering plane. The direct (line-of-sight) CEM detected both neutral and charged H particles, and the indirect (no line-of-sight) CEM detected only charged H particles. A set of electrostatic deflection plates located near the flight path to the direct CEM was used in order to separate particles according to their charge. Ion fractions were determined by measuring the TOF spectra with and without a voltage applied to the deflection plates.¹⁸ The sample was mounted on a conventional manipulator that provided reproducible rotation in both the azimuthal and incident angles within $\pm 0.5^\circ$. The temperature of the sample was measured by a calibrated infrared pyrometer and a thermocouple attached to the front edge of the sample surface. The Cu(111) single crystal from Alfa Aesar was 10 mm in diameter and 3 mm thick. The surface was mechanically polished with successively finer grits of alumina down to $0.05 \mu\text{m}$. The sample surface was cleaned in the UHV environment by 0.5 keV Ar^+ bombardment and sample annealing at 700 K. Na was evaporated from a thoroughly outgassed commercial SAES Getters source. The evaporation rate was calibrated in preliminary experiments by measuring the attenuation of the signal from 4 keV Ar^+ scattering from Cu and the saturation of the Na recoil signal. The well known exponential dependence²⁴ of the negative ion fraction on the work function was utilized to monitor Na coverage. Deposition of Na on the Cu surface induces a change in work function⁶ that leads to a pronounced increase in the scattered negative ion yield. The coverage was determined during exposure by comparison of the change in the scattered H negative ion fraction with the change in the work function versus Na coverage measurements.⁶ The resulting estimated error in the coverage is $\sim 0.01 \text{ ML}$.

Figure 1(a) shows typical experimental results for H backscattering along the $[\bar{1}2\bar{1}]$ direction from both clean and Na covered ($\theta=0.25$) Cu(111) surfaces. The $[\bar{1}2\bar{1}]$ direction was chosen because of the smaller interatomic distances between the Na and Cu atoms and hence the more obvious blocking effects.¹³ The difference (D) and ratio (R) between the normalized yields are shown in Fig. 1(b). D is defined as the normalized yield after Na exposure minus the normalized yield before Na exposure. The physical meaning of such a quantity is that for $D < 0$ ($D > 0$) in the angular range from α to $(\alpha + \delta\alpha)$, there is a decrease (increase) in the flux of scattered H particles reaching the detector after the surface is exposed to Na. Conversely, any change in the atomic pattern of the surface due to absorption of Na atoms will be revealed as nonzero D . The physical origin for a negative D arises from the fact that part of the backscattered H particles that could have reached the detector were deflected out of the detector cone by the absorbed Na atoms. Most of these deflected backscattered H particles were focused into the edge of the blocking cone leading to the corresponding positive D . At large exit angles, no positive D is observed because of the overlap between the blocking cones and the shadow cones; this is described in detail below.

A detailed analysis of the scattered particle trajectories provides the explanation of the observed transformation of

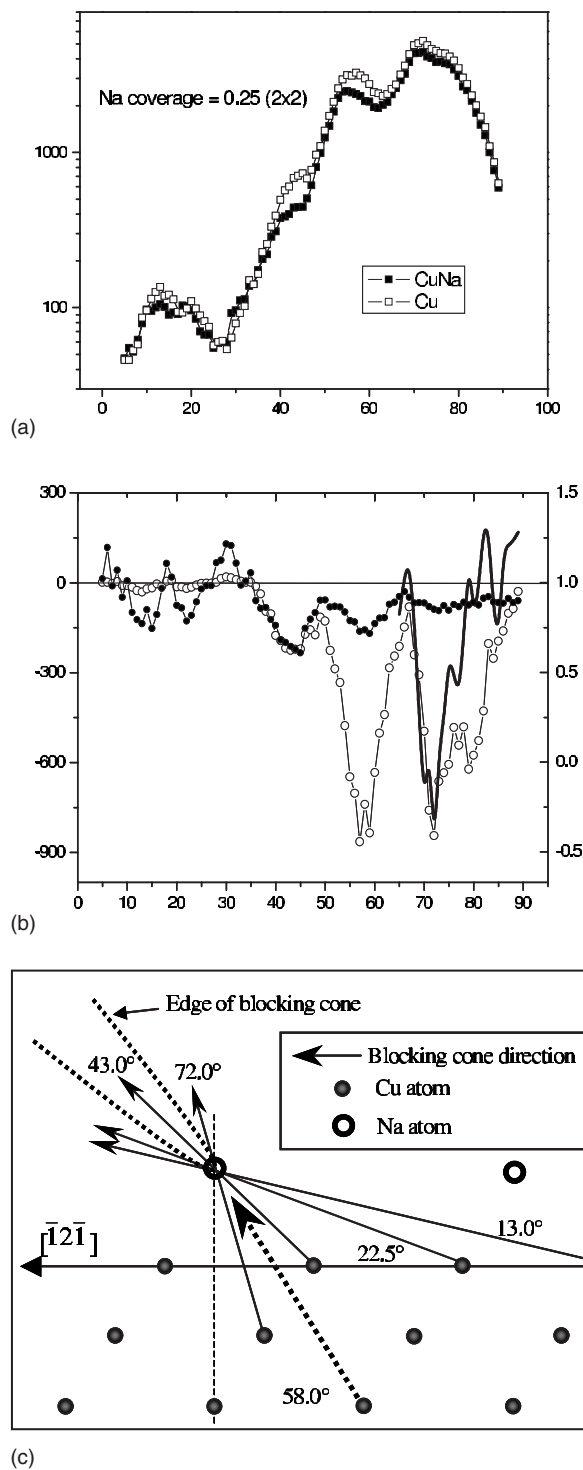


FIG. 1. Results and interpretation of incident angle scans on the Na covered ($\theta=0.25$) Cu(111) surface along the $[\bar{1}2\bar{1}]$ direction with a scattering angle of 100° . (a) The exit angle dependence of the yield of H scattered from clean Cu(111) and Na covered Cu(111) surfaces. (b) The difference and ratio of the angular distributions from Fig. 1(a) due to the presence of Na on the Cu(111) surface. The solid line is a SARIC simulation from 65° to 95° . (c) Side view of the Na/Cu(111) structure with observable blocking cone directions and the blocking cone at 43.0° . The dashed arrow shows one of the interatomic axes that does not contribute to the blocking effect.

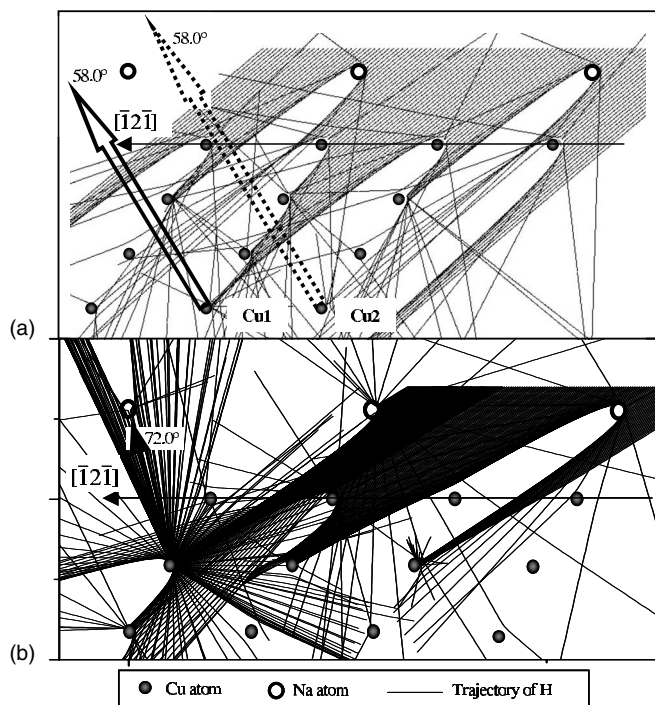


FIG. 2. MD simulation of the origination of the minima at 58.0° and 72.0° in Fig. 1. (a) The solid arrow represents high scattering intensity because the fourth-layer atom (Cu1) is in the edges of the shadow cones where incoming trajectories are focused. The dashed arrow represents lower scattering intensity from the neighboring fourth-layer atom (Cu2) because this atom is in the shadow of an adsorbed Na atom. (b) The solid arrow shows the direction of the blocking cone that is responsible for the obvious minimum at 72.0° .

the experimental angular distribution upon Na chemisorption. Figure 1(c) shows cross sections perpendicular to the Cu(111) surface along the $[\bar{1}2\bar{1}]$ azimuth with the interatomic vectors responsible for the blocking cones. The difference curve in Fig. 1(b) exhibits five minima located at 13.0° , 22.5° , 43.0° , 58.0° , and 72.0° , which can be directly associated with the interatomic directions. The features at 13.0° , 22.5° , and 43.0° are a result of H scattered from the first-layer Cu atoms and blocked by the Na atoms. Although the minimum at 58.0° corresponds to one of the interatomic directions between the Na and Cu atoms, this minimum is a result of a shadowing effect on the incoming portion of the H trajectory; the Na atom shadows half of the scattering centers. MD simulation results illustrating the origination of this minimum are shown in Fig. 2(a). For a clean Cu(111) surface, the high intensity of scattered particles at exit angle 58.0° [Fig. 1(a)] is a result of the focusing effect from shadow cones produced by the Cu atoms in the near-surface layers onto the fourth layer Cu atoms [Fig. 2(a), Cu1]. After Na adsorption on the fcc position, the shadow cones produced by Na atoms cover half of the fourth layer Cu scatters [Fig. 2(a), Cu2], which leads to the minimum at 58.0° . The minimum at 72.0° is a result of H atoms scattered from the second Cu layer and blocked by the Na atoms, as shown in Fig. 2(b). The three small minima beyond 72.0° [Fig. 1(b)] are a result of shadowing (similar to the minimum at 58.0°) and are not suitable for precise determination of the Na position.

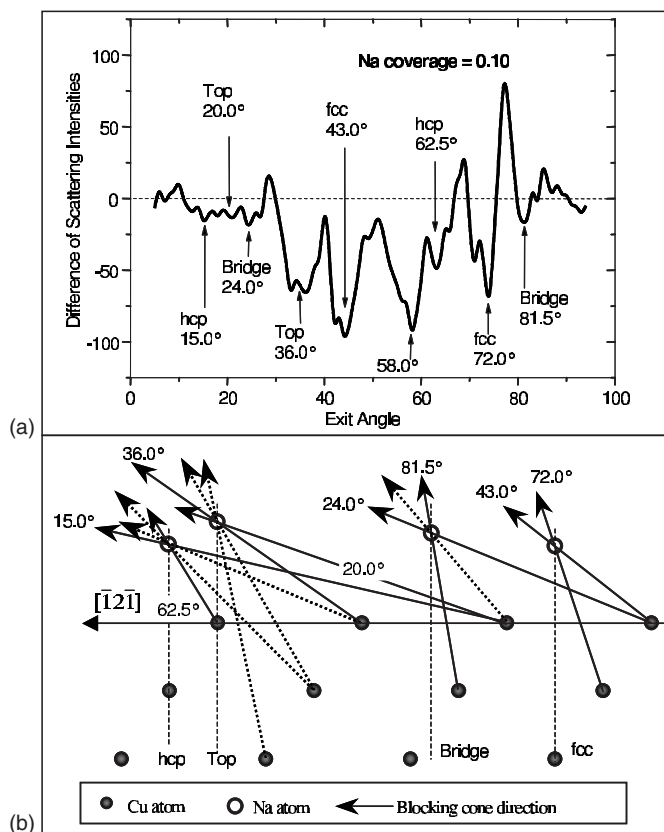


FIG. 3. Results and interpretation of the incident angle scan on Na covered ($\theta=0.10$) Cu(111) along the $[\bar{1}2\bar{1}]$ direction with scattering angle of 100° . (a) The difference in the scattering angular distributions for a clean Cu(111) surface and a Na/Cu(111) surface with $\theta=0.10$. (b) Side view of the Na/Cu(111) surface for four different Na adsorption positions. The solid arrows with numbers for the exit angles indicate the observed blocking cone directions and the dotted arrows indicate blocking cone directions that were not observed.

As shown in Fig. 1(c), four interatomic axes intersect at a single point which corresponds to the position of the Na atoms responsible for the blocking effect. It unambiguously shows that the majority of the Na atoms populate the face-centered cubic (fcc) threefold sites, in agreement with the prediction of Johan *et al.*¹⁰ Solving for the intersection of these four lines leads to a Na atom height above the first-layer Cu atoms of $2.7 \pm 0.1 \text{ \AA}$. This is larger than the calculated value of 2.40 \AA from Johan *et al.*,¹⁰ but smaller than the result of a hard sphere close-packed structure with Cu and Na radii of 1.28 and 1.91 \AA , respectively,²⁵ yielding an adsorption height of Na on the fcc Cu(111) site of 2.83 \AA . The metallic radii are used because the nearly ionic adsorbates at low coverage change to an almost neutral metallic overlayer at high coverage.^{3,4,26}

In order to provide additional proof of the interpretation of the experimental results, SARIC simulations were carried out for targets consisting of three atomic layers of Cu and scattering exit angles from 65° to 95° . Excellent agreement [Fig. 1(b), solid line] is obtained between the experimental

data and the SARIC simulation results with the following parameters: vibration amplitude: 0.05 Å, Na fcc site and Na-Cu height: 2.7 Å.

Direct evidence for the (2×2) Na structure at room temperature was not obtained because TOF-SARS probes the short-range periodicity of the surface, i.e., < 10 Å. However, the existence of the (2×2) Na structure at a coverage $\theta = 0.25$ can be predicted from the dependence of the adsorption site preference on coverage, assuming that the repulsion and uniform spacing still exists between the dipole moments of the adsorbed Na atoms.^{6,7} We should also mention that Fischer²⁶ reported Na islands rather than homogeneous distribution at this submonolayer coverage.

Figure 3 depicts the experimental result and the interpretation of the Na adsorption site at the lower coverage of θ

$= 0.10$. As shown in Fig. 3(a), at this low coverage, characteristic minima for each of the possible adsorption sites were observed. The directions of the blocking cones and the corresponding adsorption sites are shown in Fig. 3(b). The presence of adsorbed Na atoms on all of the possible adsorption positions indicates that there is no adsorption site preference at $\theta = 0.10$, which agrees with former observations.⁴⁻⁶

In conclusion, the technique of low-energy ion blocking has been successfully used to quantitatively probe the submonolayer structure of Na on a Cu(111) surface at room temperature, with analysis by simple geometrical constructs. At a coverage of $\theta = 0.25$, the fcc threefold site was found to be the preferred site for the Na atoms with a height of 2.7 ± 0.1 Å above the surface. At a lower coverage of $\theta = 0.10$, Na was found in all four possible adsorption sites.

-
- ¹H. Tochihara and S. Mizuno, *Prog. Surf. Sci.* **48**, 75 (1998).
²R. D. Diehl and R. McGrath, *Surf. Sci. Rep.* **23**, 43 (1996).
³S. A. Lindgren and L. Wallden, *Phys. Rev. B* **22**, 5967 (1980).
⁴S. A. Lindgren, C. Svensson, and L. Wallden, *Phys. Rev. B* **42**, 1467 (1990).
⁵R. Dudde, L. S. O. Johansson, and B. Reihl, *Phys. Rev. B* **44**, 1198 (1991).
⁶D. Tang, D. McIlroy, X. Shi, C. Su, and D. Heskett, *Surf. Sci.* **255**, L497 (1991).
⁷J. Kliewer and R. Berndt, *Surf. Sci.* **477**, 250 (2001).
⁸J. Kliewer and R. Berndt, *Phys. Rev. B* **65**, 035412 (2002).
⁹L. Padilla-Campos, A. Toro-Labbé, and J. Maruani, *Surf. Sci.* **24**, 385 (1997).
¹⁰J. M. Carlsson and B. Hellsing, *Phys. Rev. B* **61**, 13973 (2000).
¹¹T. Torsti, V. Lindberg, M. J. Puska, and B. Hellsing, *Phys. Rev. B* **66**, 235420 (2002).
¹²S. D. Borisova, G. G. Rusina, S. V. Eremeev, G. Benedek, P. M. Echenique, I. Y. Sklyadneva, and E. V. Chulkov, *Phys. Rev. B* **74**, 165412 (2006).
¹³J. W. Rabalais, *Principles and Applications of Ion Scattering Spectrometry* (Wiley-Interscience, New York, 2002).
¹⁴E. S. Parilis, L. M. Kishinevsky, N. Yu. Turaev, B. E. Baklitzky, F. F. Umarov, V. Kh. Verleger, and I. S. Bitensky, *Atomic Collisions on Solids* (North-Holland, New York, 1993).
¹⁵S. S. Sung, V. Bykov, A. Al-Bayati, C. Kim, S. S. Todorov, and J. W. Rabalais, *Scanning Microsc.* **9**, 321 (1995).
¹⁶V. Bykov, C. Kim, M. M. Sung, K. J. Boyd, S. S. Todorov, and J. W. Rabalais, *Nucl. Instrum. Methods Phys. Res. B* **114**, 371 (1996).
¹⁷K. M. Lui, Y. Kim, W. M. Lau, and J. W. Rabalais, *J. Appl. Phys.* **86**, 5256 (1999).
¹⁸T. Ito, I. L. Bolotin, R. Zhang, B. N. Makarenko, B. Bahrim, and J. W. Rabalais, *Surf. Sci.* **594**, 54 (2005).
¹⁹T. Ito, I. L. Bolotin, B. N. Makarenko, and J. W. Rabalais, *Surf. Sci.* **565**, 163 (2004).
²⁰A. Kutana, I. L. Bolotin, and J. W. Rabalais, *Surf. Sci.* **495**, 77 (2001).
²¹J. W. Rabalais, *Science* **250**, 521 (1990).
²²O. Grizzi, M. Shi, H. Bu, and J. W. Rabalais, *Rev. Sci. Instrum.* **61**, 740 (1990).
²³B. Bahrim, B. Makarenko, and J. W. Rabalais, *Surf. Sci.* **594**, 62 (2005).
²⁴L. Yu Ming, *Phys. Rev. Lett.* **40**, 574 (1978).
²⁵A. F. Wells, *Structural Inorganic Chemistry* (Oxford University Press, Oxford, England, 1984).
²⁶N. Fischer, S. Schuppler, Th. Fauster, and W. Steinmann, *Surf. Sci.* **314**, 89 (1994).